19th International Conference on
Adaptive Structures and Technologies
October 6-9, 2008
Ascona, Switzerland

Distributed Synthetic Jet Actuators for the Control of Nonlinear Aeroelastic Systems

Milanese, A.[1]*, De Breuker, R.[2], Marzocca, P.[1] and Abdalla, M.M.[2]
[1] Mechanical and Aeronautical Engineering Department, Clarkson University, Potsdam, NY, United States
[2] Aerospace Structures Group, Delft University of Technology, Delft, the Netherlands
* Corresponding Author: 8 Clarkson Ave., 13699-5725 Potsdam, NY, United States
Tel: +1 315 268 3887, E-mail: milanesa@clarkson.edu

ABSTRACT

Synthetic Jet Actuators (SJAs) are one of the most promising fluidic actuators for flow control. Traditionally they are used for boundary layer control, however, in the recent past, the authors have shown that they can also be used suitably for aeroelastic purposes. This is due to the fact that SJAs displace the streamlines around a lifting body, changing the aerodynamic forces and moments. In order the SJAs to be used for active real-time control, the flow field generated by these actuators needs to be described in an analytical way for fast analysis. Such an analytical model is developed based on Theodorsen's theory. The unsteady aerodynamic model stems also from Theodorsen's theory, and the structure is a two degree-of-freedom model – pitch and plunge. The structural model is nonlinear in the sense that a cubic nonlinearity is added to the torsion spring. The whole system is transformed into state space form, and the jet is used as a control input. Sliding mode control is used as a control strategy to suppress the limit cycle oscillations.

Keywords: Synthetic Jet Actuators, Nonlinear Aeroelasticity, Limit Cycle Oscillation, Sliding Mode Control

1. INTRODUCTION

Synthetic Jet Actuators (SJAs) are fluidic devices that can blow and suck air. They are conceptually simple and consist of a cavity containing a vibrating membrane that pushes flow in and out the cavity through an orifice. For aeronautical applications, piezoelectric actuation can be conveniently used. The output jet velocity can be maximized by driving the membrane at a resonant frequency of either the membrane itself or the cavity, or even the interaction between the two. A usual application of SJAs is to energize the boundary layer on a lifting surface and hence postpone flow separation. Another effect is a change of the streamline pattern around the airfoil, which is called the method of "virtual shaping". This causes a global change in aerodynamic forces and moments on the lifting surface. The flow field resulting by the use of SJAs is inherently complex, and either accurate CFD models or experimental results are needed. In spite of this, a reduced-order model to describe the change in lift and moment due to the SJAs, based on Theodorsen's formulation, has been proposed by the authors in the recent past [1]. Such an approach found its usefulness in a real-time control framework, where knowledge of the additional aerodynamic terms due to the SJA must be available instantaneously.

Previous work in the field of control of linear aeroelastic systems has shown the effectiveness of SJAs: both gust load alleviation and flutter postponement have been achieved, either separately [2,3], or simultaneously [4,5]. A transfer function based, lead-lag control has been analyzed initially [2,3,4]; then, a more refined state space LQR control methodology has been investigated [5].

The behavior of a nonlinear aeroelastic system is clearly different. For a flow velocity above the linear flutter speed, sustained oscillations in the form of Limit Cycle Oscillations (LCO) can occur instead of unbridled growth of the airfoil's pitching or plunging amplitude. The nonlinearities causing the LCO can be induced by structural or aerodynamic effects. However, in case of the typical two-dimensional airfoil aeroelastic analysis, often structural nonlinearities are used. This is also the case in the present paper.

Another novelty, described in this paper, in the research of aeroelastic control using synthetic jets is the application of a sliding mode controller. This controller is robust, for it is able to adapt to changing system dynamics and flow speed. Sliding mode control has been applied to two- and three-dimensional aeroelastic systems successfully in the past [6,7]. The SJA model itself accounts for a jet distribution of a designated part of the airfoil, and the jet can be located at various locations on the airfoil. The distribution width and jet location are investigated parametrically.

The paper is organized as follows. First the aeroelastic model, accounting for the SJA, is explained. Next the control strategy using the sliding mode controller is given, followed by the results of the design case studies. Finally, pertinent conclusions are drawn.

2. AEROELASTIC MODELING

A two-dimensional lifting surface, with plunge and pitch degrees-of-freedom, is considered. The rotational stiffness of the aeroelastic system k_α is nonlinear and depends on the pitch angle α. Such a system exhibits Limit Cycle Oscillations (LCOs) and it is chosen in order to evaluate the effectiveness of the control capabilities provided by the SJAs in a nonlinear aeroelastic setting. A sketch of the system, without the SJAs, is shown in Figure 1. The nonlinear aeroelastic governing equations, considering also the forces due to the SJAs, can be written in the time domain as:

$$\begin{bmatrix} m & S_\alpha \\ S_\alpha & I_\alpha \end{bmatrix} \begin{Bmatrix} \ddot{h} \\ \ddot{\alpha} \end{Bmatrix} + \begin{bmatrix} c_h & 0 \\ 0 & c_\alpha \end{bmatrix} \begin{Bmatrix} \dot{h} \\ \dot{\alpha} \end{Bmatrix} + \begin{bmatrix} k_h & 0 \\ 0 & k_\alpha(\alpha) \end{bmatrix} \begin{Bmatrix} h \\ \alpha \end{Bmatrix} = \begin{Bmatrix} -\left(L + L_{vj}\right) \\ \left(M + M_{vj}\right) \end{Bmatrix} \tag{1}$$

where m, I_α, S_α , c_h, c_α, k_h and k_α are standard structural mass, damping and stiffness parameters, L and M are the aerodynamic lift and moment due to the degrees-of-freedom motions, while L_{vj} and M_{vj} are the control contributions due to the SJAs.

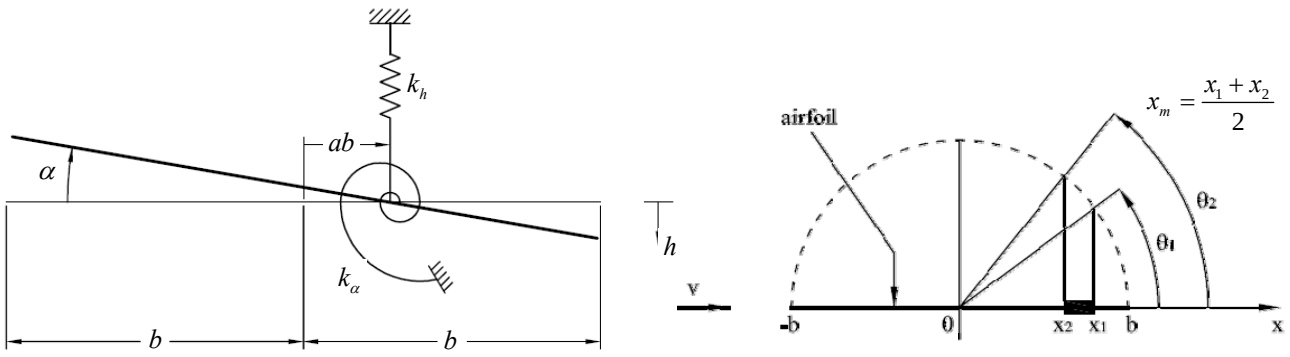

Figure 1: Sketch of a) the plunge and pitch aeroelastic system, and b) the distributed jet on the airfoil.

If the fluid is assumed to be incompressible and irrotational, and if the airfoil is considered thin, the unsteady aerodynamic forces due to the plunge h and pitch α displacements can be described in the Laplace domain using Theodorsen's formulation [8]. In particular, the lift L is given by:

$$-\hat{L} = -\rho b^2 v\pi s\hat{\alpha} - \rho b^2 \pi s^2 \hat{h} + \rho b^3 \pi a s^2 \hat{\alpha} - 2\pi\rho v b C\left(\frac{sb}{v}\right)\left[v\hat{\alpha} + s\hat{h} + b\left(\frac{1}{2} - a\right)s\hat{\alpha} \right] \tag{2}$$

where ρ is the air density, a is the dimensionless location of the elastic axis, b is the semi-chord, s is the Laplace variable, v is the free stream flow velocity and C is Theordorsen's function. The hat notation is introduced to distinguish between functions in the time or Laplace domain. When it comes to modern control strategy development, it is usually convenient to use a time domain representation and a corresponding state-space formulation. Using the Jones rational approximation the Theodorsen function is conveniently expressed as [9]:

$$C\left(\frac{sb}{v}\right) \cong 1 - \frac{0.165s}{s + 0.0455\frac{v}{b}} - \frac{0.335s}{s + 0.3\frac{v}{b}} \tag{3}$$

To conveniently describe the circulatory component of the unsteady aerodynamic forces, the following aerodynamic lag states can be introduced:

$$\begin{aligned}
&\hat{a}_1 = \frac{0.165s}{s + 0.0455\frac{v}{b}}\hat{\alpha}, \quad \hat{a}_2 = \frac{0.335s}{s + 0.3\frac{v}{b}}\hat{\alpha}, \qquad \hat{a}_3 = \frac{0.165s}{s + 0.0455\frac{v}{b}}s\hat{h} \\
&\hat{a}_4 = \frac{0.335s}{s + 0.3\frac{v}{b}}s\hat{h}, \qquad \hat{a}_5 = \frac{0.165s}{s + 0.0455\frac{v}{b}}s\hat{\alpha}, \quad \hat{a}_6 = \frac{0.335s}{s + 0.3\frac{v}{b}}s\hat{\alpha}
\end{aligned} \tag{4}$$

The above equations can be straightforwardly transformed back in the time domain.

Similarly, the unsteady aerodynamic moment is given by:

$$\begin{aligned}
\hat{M} = &-\rho b^3 v\pi\left(\frac{1}{2} - a\right)s\hat{\alpha} - \rho b^4 \pi\left(\frac{1}{8} + a^2\right)s^2\hat{\alpha} + \rho b^3 \pi a s^2 \hat{h} + \\
&+ 2\pi\rho v b^2\left(\frac{1}{2} + a\right)C\left(\frac{sb}{v}\right)\left[v\hat{\alpha} + s\hat{h} + b\left(\frac{1}{2} - a\right)s\hat{\alpha} \right]
\end{aligned} \tag{5}$$

Also in this case, the circulatory contributions of the aerodynamic moment can be expressed in the time domain using the same aerodynamic lag states a_1 to a_6 defined in Eq. (4).

The additional contributions to the lift L_{vj}, and moment, M_{vj}, due to distributed SJAs have been derived elsewhere [1, 5]:

$$\frac{\hat{L}_{vj}}{\hat{v}_j} = -\int_{\theta_1}^{\theta_2} v\rho b \sin(\theta_0)\left[C\left(\frac{sb}{v}\right)\arctan\left(\frac{\theta_0}{2}\right) + \frac{sb}{v}\sin(\theta_0) \right] d\theta_0 \tag{6}$$

$$\frac{\hat{M}_{vj}}{\hat{v}_j} = \int_{\theta_1}^{\theta_2} \frac{1}{4} b^2 v\rho \sin(\theta_0)\left[2\left(C\left(\frac{sb}{v}\right) - 1\right)\arctan\left(\frac{\theta_0}{2}\right) + 4\sin(\theta_0) - \frac{sb}{u}\sin(2\theta_0) \right] d\theta_0 - \frac{\hat{L}_{vj}}{\hat{v}_j} ab \tag{7}$$

where v_j is the jet velocity. These additional lift and moment can be expressed in the time domain by using the same rational fraction approximation for the Theodorsen function. It is convenient to define two additional lag states, as follows:

$$\hat{a}_7 = \frac{0.165s}{s + 0.0455\frac{v}{b}}\hat{v}_j, \quad \hat{a}_8 = \frac{0.355s}{s + 0.3\frac{v}{b}}\hat{v}_j \tag{8}$$

With the above equations, it is now possible to develop a state-space model for the nonlinear aeroelastic system controlled by the distributed SJAs. The evolution of the system is described by a set of first order differential equations, as follows:

$$\dot{\mathbf{x}} = \mathbf{A(x)x} + \mathbf{Bu} \tag{9}$$

The state vector **x** has 13 components, as follows:

$$\mathbf{x} = \begin{bmatrix} h & \alpha & \dot{h} & \dot{\alpha} & a_1 & a_2 & a_3 & a_4 & a_5 & a_6 & v_j & a_7 & a_8 \end{bmatrix}^T \tag{10}$$

The input vector **u** in this case is a scalar, and it is taken as the time derivative of the jet velocity v_j:

$$\mathbf{u} = \dot{v}_j \tag{11}$$

The matrix **A(x)** is not constant, but depends on the states **x**, since a nonlinear torsion spring is introduced. Both the matrix **A(x)** and the vector **B** are reported for completeness in the Appendix.

3. SLIDING MODE CONTROLLER

Sliding mode controllers are part of the family of variable structure control systems. The basic idea behind the controller strategy is rather simple and quite powerful. A short description with regards to the regulation problem is provided here, with the resulting control law equations used in the analysis. More information, with historical background, rigorous mathematical details and examples, can be found in [10].

Consider a dynamic system with two states, x_1 and x_2. The trajectories can then be visualized on a plane. With reference to Figure 2 consider a line through the origin in the state space. For this two-dimensional system, such a line is the desired *sliding surface* L_s. The sliding mode controller is designed so that:

- starting from an arbitrary configuration, the system evolves towards and reaches the sliding surface in a finite time t_s;
- for all successive times, $t > t_s$, the controller keeps the states on the sliding surface, hence *ideal sliding motion* takes places, asymptotically tending to the origin.

In this aeroelastic application, the states vector **x** has thirteen components. The straight line of Fig. 2 becomes a hyper-plane in a higher-dimensional space, but it can still be described by a vector **S**.

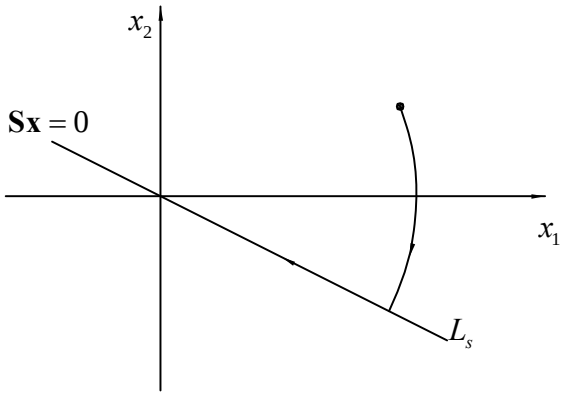

Figure 2: Example of action of sliding mode controller on a system with 2 states.

Such a control strategy presents various advantages, among which robustness towards parameters uncertainties: if the underlying system changes its properties, the controller tries (within certain limits) to guide the states towards the sliding surface L_s and to keep them there, since the feedback action depends on the distance from the sliding surface and not on the parameters of the system.

Next, the steps followed to design the controller are reported. The first one is to identify an underlying linear system. In this case, since the only nonlinearity is given by the nonlinear torsional spring $k_\alpha(\alpha)$, a natural choice is to consider the linear system obtained by linearizing k_α around $\alpha = 0$. Hence, the matrix **A(x)** of Eq. (9) can be divided in a constant linear part, and in a nonlinear one, as follows:

$$\mathbf{A(x)} = \mathbf{A_l} + \mathbf{A_{nl}}(\mathbf{x}) \tag{12}$$

The next step is to bring the underlying linear system to regular form. This is accomplished by a change of coordinate system, from states **x** to **z**, through a rotation matrix $\mathbf{T_r}$, such that

$$\mathbf{z} = \mathbf{T_r x}, \qquad \mathbf{T_r A_l T_r^T} = \begin{bmatrix} \mathbf{A_{11}} & \mathbf{A_{12}} \\ \mathbf{A_{21}} & \mathbf{A_{22}} \end{bmatrix}, \qquad \mathbf{T_r B} = \begin{bmatrix} \mathbf{0} \\ \mathbf{B_2} \end{bmatrix} \tag{13}$$

The dynamic of such a linear system is hence described by:

$$\begin{cases} \dot{\mathbf{z}}_1 = \mathbf{A_{11}} \mathbf{z}_1 + \mathbf{A_{12}} \mathbf{z}_2 \\ \dot{\mathbf{z}}_2 = \mathbf{A_{21}} \mathbf{z}_1 + \mathbf{A_{22}} \mathbf{z}_2 + \mathbf{B_2 u} \end{cases} \tag{14}$$

Having recast the equations in these terms, the input **u** acts directly only on a subset of the states.

The switching function s that identifies the sliding surface is also transferred in the new coordinates as follows:

$$s = \mathbf{Sx} \quad \rightarrow \quad s = \mathbf{S_1 z_1} + \mathbf{S_2 z_2}, \qquad \mathbf{S T_r^T} = \begin{bmatrix} \mathbf{S_1} & \mathbf{S_2} \end{bmatrix} \tag{15}$$

After the ideal sliding motion takes place ($t > t_s$), the system obeys to a reduced order dynamics. In fact, since the states are confined to stay on L_s, it is readily found that:

$$\mathbf{S_1 z_1} + \mathbf{S_2 z_2} = 0 \quad \rightarrow \quad \mathbf{z_2} = \mathbf{M z_1}, \qquad \mathbf{M} = \mathbf{S_2^{-1} S_1} \tag{16}$$

Hence, the states $\mathbf{z_2}$ follow (statically) the states $\mathbf{z_1}$, whose evolution is dictated by:

$$\dot{\mathbf{z}}_1 = \left(\mathbf{A}_{11} - \mathbf{A}_{12}\mathbf{M}\right)\mathbf{z}_1 \tag{17}$$

The sliding surface, described by **S**, ultimately shapes the dynamics of the sliding motion, through **M**.

The next step is therefore the design of the sliding surface itself. Several approaches are possible, among which quadratic minimization of a cost function, eigenvalue placement and eigenstructure assignment methods [10]. In this work, the quadratic minimization approach is chosen. The problem becomes that of choosing **M** (and **S**) such that the functional

$$J = \int_{t_s}^{\infty} \mathbf{x}^{\mathrm{T}}\mathbf{Q}\mathbf{x}dt \tag{18}$$

is minimized. The solution can be found using standard LQR techniques. Physically, this approach accounts for stabilizing the system after the sliding motion takes place ($t > t_s$) as fast as possible, assigning proper weights to the different states through the matrix **Q**. The choice of the **Q** is somehow arbitrary: in this work the same weights are assigned to the three states h, α and v_j, while a zero weight is assigned to the remaining ones.

This approach assumes that all the states of the system are available for feedback. In this application, however, this is not the case, as in particular the lagged aerodynamic states are not easily accessible. Hence, the sliding surface **S** is modified by setting to zero various components, as follows:

$$\mathbf{S} = [\underbrace{* \ *}_{h,\alpha} \ \underbrace{0 \ 0}_{\dot{h},\dot{\alpha}} \ \underbrace{0 \ 0 \ 0 \ 0 \ 0 \ 0}_{a_1 \text{ to } a_6} \ \underbrace{*}_{v_j} \ \underbrace{0 \ 0}_{a_7, a_8}] \tag{19}$$

In the above, a star in a certain position indicates that the optimal value assigned to **S** through LQR minimization is kept unchanged. With such a modification, the feedback law is *de facto* acting only on h, α and v_j, that can be considered to be known outputs of the system. The plunge and pitch velocities and the various lagged aerodynamic states do not appear in the feedback loop.

The last step is to obtain the control law. The control signal **u** is given by [10]:

$$\mathbf{u} = (\mathbf{SB})^{-1}\left(\mathbf{\Phi S} - \mathbf{SA}_1\right)\mathbf{x} \tag{20}$$

where $\mathbf{\Phi}$ in this case is a scalar dictating how fast the sliding surface is reached in the initial phase of the control ($t < t_s$). Since in this application **u** has the physical meaning of time derivative of v_j, the signal to be sent to the actuator can be readily obtained by integration.

Table 1 Aeroelastic system properties

mass m	12.387 [kg/m]	plunge stiffness k_h	2844.4 [N/m/m]
inertia I_α	0.065 [kg·m^2/m]	pitch damping c_α	0.036 [N·m/(1/s)/m]
static moment S_α	0.1097 [kg·m/m]	plunge damping c_h	27.43 [N/(m/s)/m]
semi-chord b	0.135 [m]	air density ρ	1.225 [kg/m^3]
shear center a	–0.8424 [/]	free stream velocity v	15 [m/s]
pitch stiffness k_α	$2.820 - 62.322\,\alpha + 3709.71\,\alpha^2 - 24195.6\,\alpha^3 + 48757.0\,\alpha^4$ [N·m/m]		

4. RESULTS

For the numerical computations, a set of parameters similar to the ones of [11] is used. Table 1 summarizes the system properties. A disturbance is introduced in the system as a non-zero initial condition, with an initial plunge and pitch displacements equal to $h_0 = -0.001$ m and $\alpha_0 = 0.09$ rad, respectively. The simulation is performed in the time domain, using the variable order Adams-Bashforth-Moulton integrator as implemented in the MATLAB® function `ODE113` [12].

All the simulations are performed at a free stream velocity v equal to 15 m/s. At this speed, the open-loop nonlinear system exhibits an LCO, as shown in Figure 3.

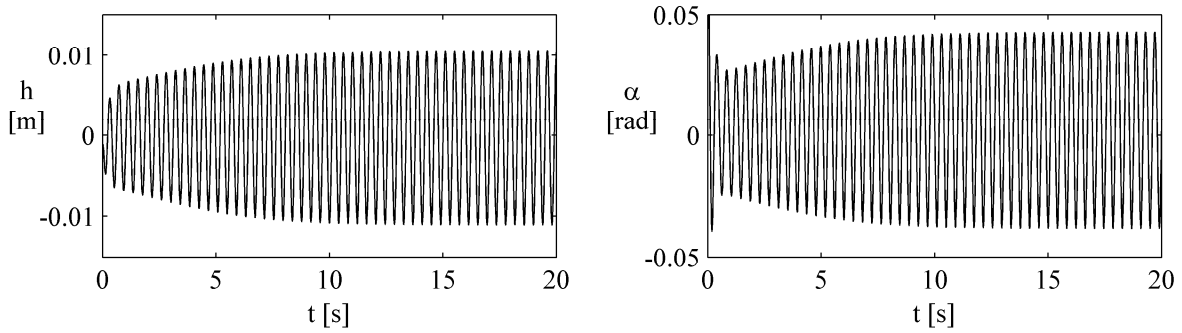

Figure 3: Plunge and pitch response of the open loop system, showing the evolution towards an LCO.

The sliding mode controller is able to successfully suppress the LCO, as evident from the next figures. The feedback control law proposed here uses only the information from the plunge displacement h, the pitch rotation α and jet velocity v_j. Hence, the trajectories of these states evolve towards a sliding surface and then tend to the origin. A typical response is shown in a three dimensional plot (h, α, v_j) in Figure 4. To show the effectiveness of the control, first an initial time is given to the system to evolve in open-loop towards an LCO. No control input is used during this phase, that is, the jet velocity is zero, and the states h and α stay on a horizontal plane. When the control is turned on, the system tends to the inclined surface, that in this case represents the sliding surface. Once this is reached, the system dynamics is constrained to remain on that plane, and the states wind up towards the origin. Stabilization is therefore attained.

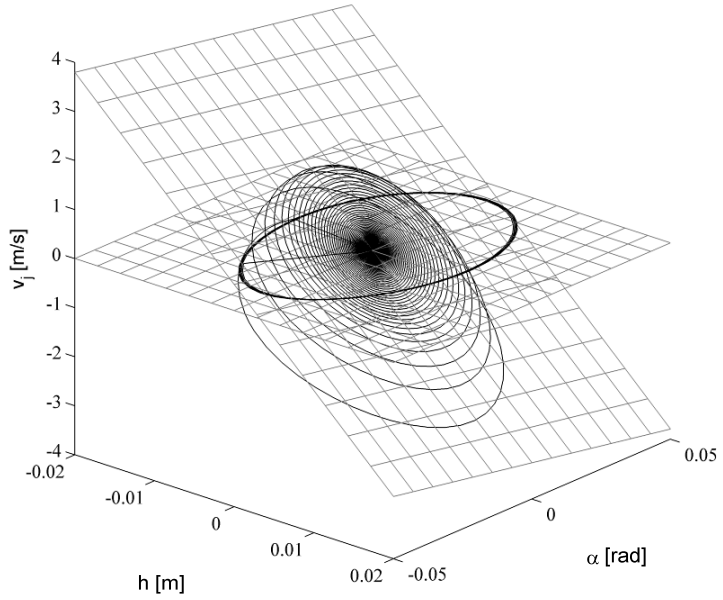

Figure 4: Three-dimensional plot of the plunge, pitch response and jet velocity v_j for the closed-loop configuration with $x_m = 0.60$, jet width 10% of the chord. The plane $v_j = 0$ and the sliding plane are shown.

Figure 5 reports a parametric analysis obtained fixing the distributed jet width to 10% of the

chord, and varying its position from leading edge to trailing edge. Since the same steps are used in designing the sliding mode controller, such an analysis leads to the conclusion that – for these particular set of system parameters – a location towards the trailing edge is more convenient. In fact, positioning the jet almost at the leading edge damps the oscillations rather slowly. Moving the SJA towards the trailing edge, the pitch rotation is damped out rather effectively. The plunge displacements are not shown in the figure, since they follow closely the pitch rotations. Out of the different configurations analyzed in Figure 5, the jet at x_m = 0.60 is the one that gives the best stabilization with the smallest jet velocity expenditure.

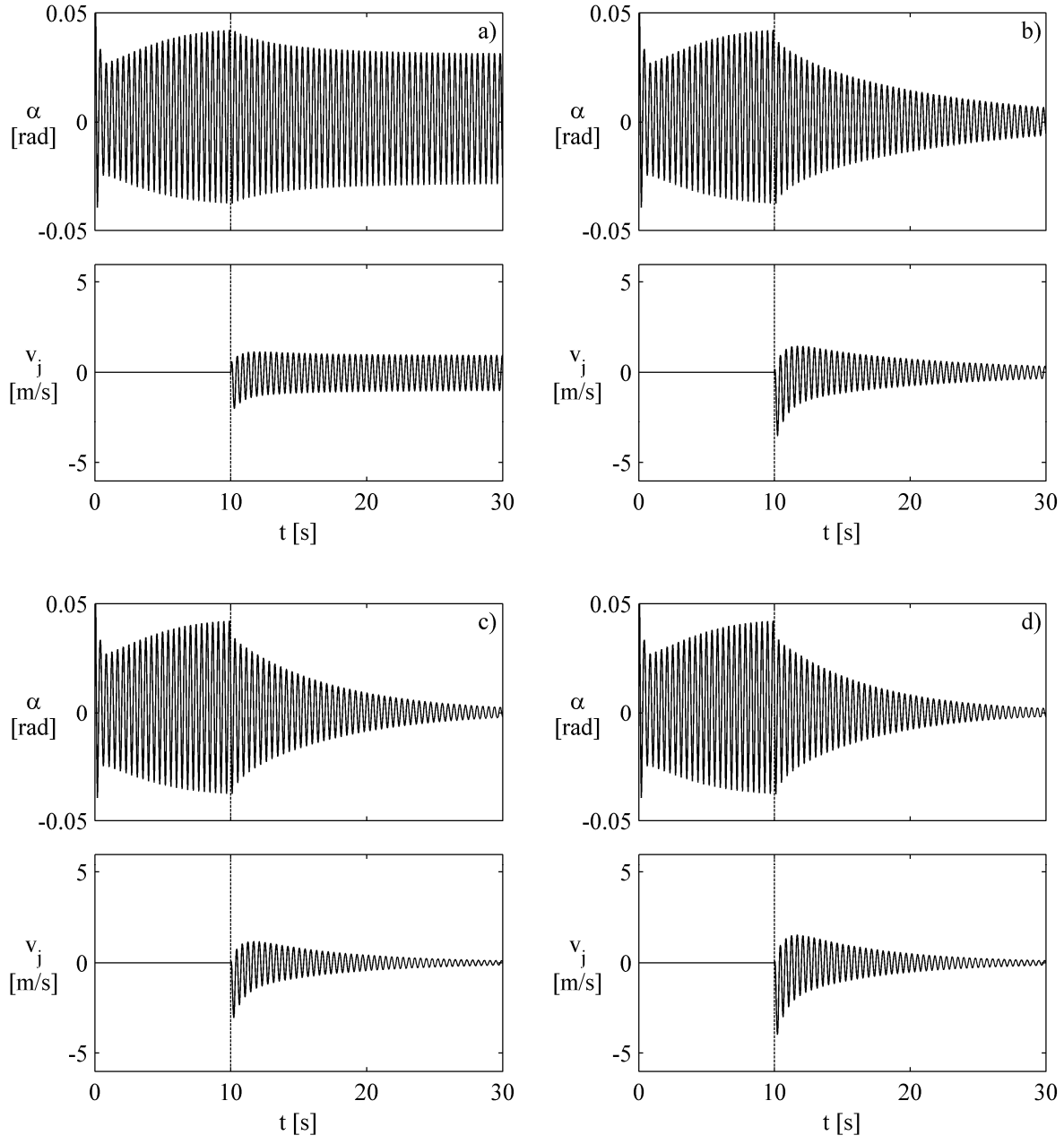

Figure 5: Pitch response and jet velocity v_j for different closed loop configurations. The distributed jet width is 10% of the chord, its position is varied: a) x_m = 0.15 (almost L.E.), b) x_m = 0.30, c) x_m = 0.60, d) x_m = 0.85 (almost T.E.).

The effect of the distributed jet width is now analyzed in Figure 6, where the distributed synthetic jet position is held constant at x_m = 0.60. The pitch response in depicted in the plots. The results in terms of stabilization effectiveness are undistinguishable between the 5% and 15% width cases. The difference is only in terms of required jet velocity v_j, that scales in an inverse proportion to

the jet width, as expected.

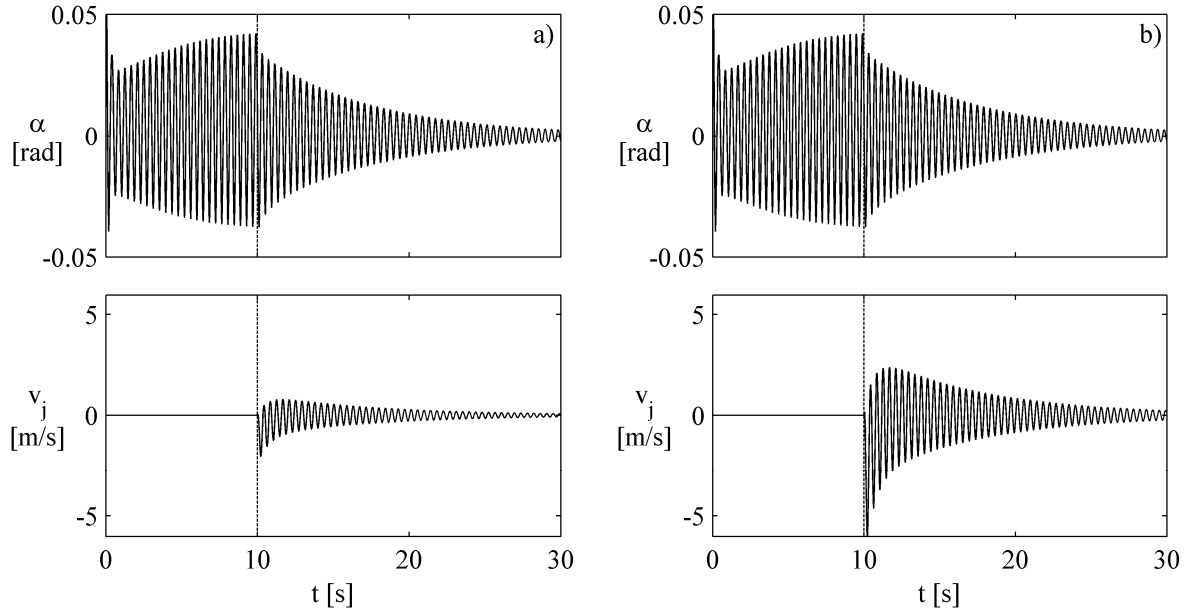

Figure 6: Pitch response and jet velocity v_j for different closed-loop configuration. The position of the jet is held constant at $x_m = 0.60$, its width is varied: a) jet width 15% of the chord, b) jet width 5% of the chord.

Finally, the robustness of the closed-loop system is assessed. In this case, a jet location $x_m = 0.60$ and jet width equal to 10% of the chord are considered. The control law is computed at the nominal pitch stiffness k_α given in Table 1. Then, the aeroelastic system is modified, by means of a reduction in the pitching stiffness k_α by 25%. A limit cycle oscillation with larger amplitude is expected. The controller, however, is still able to stabilize the system, with performances comparable to the nominal case, as shown in Figure 7. This robustness is also observed with respect to changes in other system parameters, in particular when the free stream velocity v is varied.

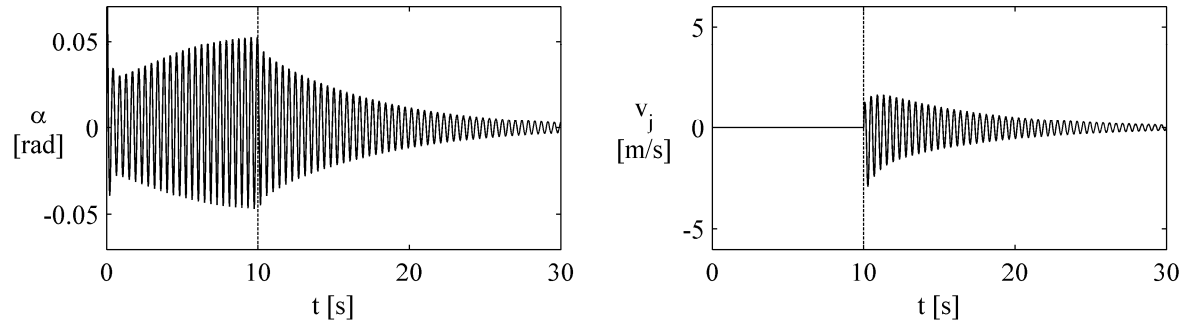

Figure 7: Pitch response and jet velocity v_j for a closed loop configuration with a reduced pitch stiffness. The position of the jet is $x_m = 0.60$, its width is 10% of the chord.

5. CONCLUSIONS

A nonlinear aeroelastic model accounting for the aerodynamic effect of Synthetic Jet Actuators has been developed. This model is used to carry out aeroelastic control studies on a typical aeroelastic section using the jet as a controller. The control strategy used is a sliding mode controller. It is shown that a SJA can indeed reduce the LCO amplitude, or even cancel it out completely. A jet situated towards the trailing edge of the airfoil proves to be more effective than the ones located more

towards the leading edge. This is in correspondence with what the authors have found in recent research efforts for linear aeroelastic systems. If the SJA distribution is made wider, and the same control performance is required, it is shown that the jet blowing velocity is reduced compared to the smaller jets. In the future, experimental work will be carried out to validate the results of the active aeroelastic control results using Synthetic Jet Actuators.

ACKNOWLEDGEMENTS

A. Milanese acknowledges the MAE Department at Clarkson University for providing partial support for this research through a Teaching Assistantship.

REFERENCES

1. Schober, S., Marzocca, P., De Breuker, R., Abdalla, M., "Reduced Order Models for Synthetic Jet Actuators on a Lifting Surface for Optimization and Control", *Proceedings of the 47th AIAA/ASME/ASCE/AHS/ASC Structures, Structural Dynamics, and Materials Conference*, Newport, RI, May 2006.
2. De Breuker, R., Abdalla, M., Marzocca, P., Gürdal, Z., "Flutter Suppression using Synthetic Jet Actuators: The Typical Section," *Proceedings of the 17th International Conference on Adaptive Structures and Technologies*, Taipei, Taiwan, October 2006.
3. De Breuker, R., Abdalla, M., Marzocca, P., "Aeroelastic Control and Load Alleviation using Optimally Distributed Synthetic Jet Actuators", *Proceedings of the 48th AIAA/ASME/ASCE/AHS/ASC Structures, Structural Dynamics, and Materials Conference*, Honolulu, HI, April 2007.
4. De Breuker, R., Milanese, A., Abdalla, M., Marzocca, P., "Simultaneous flutter suppression and load alleviation using multiple optimally distributed synthetic jet actuators," *Proceedings of the 18th International Conference on Adaptive Structures and Technologies*, Ottawa, Canada, October 2007.
5. De Breuker, R., Abdalla, M., Milanese, A., Marzocca, P., "Optimal control of aeroelastic systems using synthetic jet actuators," *Proceedings of the 49th AIAA/ASME/ASCE/AHS/ASC Structures, Structural Dynamics, and Materials Conference*, Schaumburg, IL, April 2008.
6. Na, S., Librescu, L., Kim, M.H., Jeong, I.J., Marzocca, P., "Robust aeroelastic control of flapped wing systems using a sliding mode observer," *Aerospace Science and Technology*, Vol. 10, No. 3, 2006.
7. Kim, K., Bong, K., Yoon, G., Na, S., Marzocca, P., Milanese, A., Librescu, L. (in memory), "Comparative analysis of control performances applied to a 3-DOFs nonlinear supersonic lifting surface," *Proceedings of the 49th AIAA/ASME/ASCE/AHS/ASC Structures, Structural Dynamics, and Materials Conference*, Schaumburg, IL, April 2008.
8. Theodorsen, T., "General theory of aerodynamic instability and the mechanism of flutter," *Tech. Rep. 496, NASA*, 1935.
9. Fung, Y.C., "An introduction to the theory of Aeroelasticity," Wiley, New York, 1955.
10. Edwards, C., Spurgeon, S.H., "Sliding Model Control: Theory and Applications," Taylor & Francis, London, UK, 1998.
11. Block, J.J., Strganac, T.W., "Applied active control for a nonlinear aeroelastic structure," *Journal of Guidance, Control and Dynamics*, Vol. 21, No. 6, 1998.
12. MATLAB® User's Guide, 2006, The MathWorks Inc.

APPENDIX

The matrices and vectors appearing in the state-space formulation of Eq. (9) are presented. It is first convenient to define the following three integrals, linked to the control forces contributions, expressed in terms of lift and aerodynamic moment coming from the distributed jet:

$$
\begin{aligned}
I_1 &= \int_{\theta_1}^{\theta_2} \sin\left(\theta_0\right) \arctan\left(\frac{\theta_0}{2}\right) d\theta_0 \\
I_2 &= \int_{\theta_1}^{\theta_2} \sin^2\left(\theta_0\right) d\theta_0 = \frac{1}{2}\left[\theta_2 - \theta_1 + \frac{1}{2}\sin\left(2\theta_1\right) - \frac{1}{2}\sin\left(2\theta_2\right)\right] \\
I_3 &= \int_{\theta_1}^{\theta_2} \sin^2\left(\theta_0\right) \cos\left(\theta_0\right) d\theta_0 = \frac{1}{3}\left[\sin^3\left(\theta_2\right) - \sin^3\left(\theta_1\right)\right]
\end{aligned}
\tag{A.1}
$$

For the integral I_1, no analytical solution could be found and the usual trapezoidal quadrature is used. Then, the following intermediate variables can be defined:

$$
\tilde{\mathbf{M}} = \begin{bmatrix}
0 & 0 & \tilde{m}_{1,3} & \tilde{m}_{1,4} & 0 & 0 & 0 & 0 & 0 & 0 & 0 & 0 & 0 \\
0 & 0 & \tilde{m}_{2,3} & \tilde{m}_{2,4} & 0 & 0 & 0 & 0 & 0 & 0 & 0 & 0 & 0 \\
1 & 0 & 0 & 0 & 0 & 0 & 0 & 0 & 0 & 0 & 0 & 0 & 0 \\
0 & 1 & 0 & 0 & 0 & 0 & 0 & 0 & 0 & 0 & 0 & 0 & 0 \\
0 & \gamma_1 & 0 & 0 & 1 & 0 & 0 & 0 & 0 & 0 & 0 & 0 & 0 \\
0 & \gamma_2 & 0 & 0 & 0 & 1 & 0 & 0 & 0 & 0 & 0 & 0 & 0 \\
0 & 0 & \gamma_1 & 0 & 0 & 0 & 1 & 0 & 0 & 0 & 0 & 0 & 0 \\
0 & 0 & \gamma_2 & 0 & 0 & 0 & 0 & 1 & 0 & 0 & 0 & 0 & 0 \\
0 & 0 & 0 & \gamma_1 & 0 & 0 & 0 & 0 & 1 & 0 & 0 & 0 & 0 \\
0 & 0 & 0 & \gamma_2 & 0 & 0 & 0 & 0 & 0 & 1 & 0 & 0 & 0 \\
0 & 0 & 0 & 0 & 0 & 0 & 0 & 0 & 0 & 0 & 1 & 0 & 0 \\
0 & 0 & 0 & 0 & 0 & 0 & 0 & 0 & 0 & 0 & \gamma_1 & 1 & 0 \\
0 & 0 & 0 & 0 & 0 & 0 & 0 & 0 & 0 & 0 & \gamma_2 & 0 & 1
\end{bmatrix}
\tag{A.2}
$$

$$
\tilde{m}_{1,3} = m + \rho b^2 \pi,\ \tilde{m}_{1,4} = S_\alpha - \rho \mathrm{b}^3 \pi a,\ \tilde{m}_{2,3} = S_\alpha - \rho \mathrm{b}^3 \pi a,\ \tilde{m}_{2,4} = \mathrm{I}_\alpha + \rho b^4 \pi \left(\frac{1}{8} + a^2\right)
\tag{A.3}
$$

$$
\gamma_1 = -0.165,\ \gamma_2 = -0.335
$$

$$\tilde{\mathbf{A}}=\begin{bmatrix}
\tilde{a}_{1,1} & \tilde{a}_{1,2} & \tilde{a}_{1,3} & \tilde{a}_{1,4} & \tilde{a}_{1,5} & \tilde{a}_{1,6} & \tilde{a}_{1,7} & \tilde{a}_{1,8} & \tilde{a}_{1,9} & \tilde{a}_{1,10} & \tilde{a}_{1,11} & \tilde{a}_{1,12} & \tilde{a}_{1,13} \\
0 & \tilde{a}_{2,2} & \tilde{a}_{2,3} & \tilde{a}_{2,4} & \tilde{a}_{2,5} & \tilde{a}_{2,6} & \tilde{a}_{2,7} & \tilde{a}_{2,8} & \tilde{a}_{2,9} & \tilde{a}_{2,10} & \tilde{a}_{2,11} & \tilde{a}_{2,12} & \tilde{a}_{2,13} \\
0 & 0 & 1 & 0 & 0 & 0 & 0 & 0 & 0 & 0 & 0 & 0 & 0 \\
0 & 0 & 0 & 1 & 0 & 0 & 0 & 0 & 0 & 0 & 0 & 0 & 0 \\
0 & 0 & 0 & 0 & \delta_1 & 0 & 0 & 0 & 0 & 0 & 0 & 0 & 0 \\
0 & 0 & 0 & 0 & 0 & \delta_2 & 0 & 0 & 0 & 0 & 0 & 0 & 0 \\
0 & 0 & 0 & 0 & 0 & 0 & \delta_1 & 0 & 0 & 0 & 0 & 0 & 0 \\
0 & 0 & 0 & 0 & 0 & 0 & 0 & \delta_2 & 0 & 0 & 0 & 0 & 0 \\
0 & 0 & 0 & 0 & 0 & 0 & 0 & 0 & \delta_1 & 0 & 0 & 0 & 0 \\
0 & 0 & 0 & 0 & 0 & 0 & 0 & 0 & 0 & \delta_2 & 0 & 0 & 0 \\
0 & 0 & 0 & 0 & 0 & 0 & 0 & 0 & 0 & 0 & 0 & 0 & 0 \\
0 & 0 & 0 & 0 & 0 & 0 & 0 & 0 & 0 & 0 & 0 & \delta_1 & 0 \\
0 & 0 & 0 & 0 & 0 & 0 & 0 & 0 & 0 & 0 & 0 & 0 & \delta_2
\end{bmatrix} \tag{A.4}$$

$$\tilde{a}_{1,1}=-k_h,\ \tilde{a}_{1,2}=-2\pi\rho v^2 b,\ \tilde{a}_{1,3}=-c_h-2\pi\rho v b,\ \tilde{a}_{1,4}=-\rho b^2 v\pi-2\pi\rho v b^2\left(\frac{1}{2}-a\right)$$

$$\tilde{a}_{1,5}=\tilde{a}_{1,6}=2\pi\rho v^2 b,\ \tilde{a}_{1,7}=\tilde{a}_{1,8}=2\pi\rho v b,\ \tilde{a}_{1,9}=\tilde{a}_{1,10}=2\pi\rho v b^2\left(\frac{1}{2}-a\right)$$

$$\tilde{a}_{1,11}=-v\rho b I_1,\ \tilde{a}_{1,12}=\tilde{a}_{1,13}=v\rho b I_1,\ \tilde{a}_{2,2}=-k_\alpha(\alpha)+2\rho v^2 b^2\pi\left(\frac{1}{2}+a\right)$$

$$\tilde{a}_{2,3}=2\rho v b^2\pi\left(\frac{1}{2}+a\right),\ \tilde{a}_{2,4}=-c_\alpha-\rho b^3\pi\left(\frac{1}{2}-a\right)v+2\rho v b^3\pi\left(\frac{1}{2}+a\right)\left(\frac{1}{2}-a\right) \tag{A.5}$$

$$\tilde{a}_{2,5}=\tilde{a}_{2,6}=2\rho v^2 b^2\pi\left(\frac{1}{2}+a\right),\ \tilde{a}_{2,7}=\tilde{a}_{2,8}=2\rho v b^2\pi\left(\frac{1}{2}+a\right)$$

$$\tilde{a}_{2,9}=\tilde{a}_{2,10}=2\rho v b^3\pi\left(\frac{1}{2}+a\right)\left(\frac{1}{2}-a\right),\ \tilde{a}_{2,11}=b^2 v\rho I_2+a v\rho b^2 I_1$$

$$\tilde{a}_{2,12}=\tilde{a}_{2,13}=-\frac{1}{2}b^2 v\rho I_1-a v\rho b^2 I_1,\ \delta_1=-0.0455\frac{v}{b},\ \delta_2=-0.3\frac{v}{b}$$

$$\tilde{B}=\begin{bmatrix}\tilde{b}_1 & \tilde{b}_2 & 0 & 0 & 0 & 0 & 0 & 0 & 0 & 0 & 1 & 0 & 0\end{bmatrix}^T \tag{A.6}$$

$$\tilde{b}_1=-\rho b^2 I_2,\ \tilde{b}_2=-\frac{1}{2}b^3\rho I_3+a\rho b^3 I_2 \tag{A.7}$$

Finally, the matrix **A** and the vector **B** appearing in Eq. (9) can be found as:

$$\mathbf{A}=\tilde{\mathbf{M}}^{-1}\tilde{\mathbf{A}} \tag{A.8}$$

$$\mathbf{B}=\tilde{\mathbf{M}}^{-1}\tilde{\mathbf{B}} \tag{A.9}$$